Neuropharmacology 191 (2021) 108560

Contents lists available at ScienceDirect

Neuropharmacology

journal homepage: www.elsevier.com/locate/neuropharm

Optogenetic induction of orbitostriatal long-term potentiation in the dorsomedial striatum elicits a persistent reduction of alcohol-seeking behavior in rats

Yifeng Cheng [a,b], Xueyi Xie [a], Jiayi Lu [a], Himanshu Gangal [a], Wei Wang [a], Sebastian Melo [a], Xuehua Wang [a], Jared Jerger [a], Kayla Woodson [a], Eric Garr [b], Yufei Huang [a], Patricia Janak [b], Jun Wang [a,*]

[a] Department of Neuroscience and Experimental Therapeutics, College of Medicine, Texas A&M University Health Science Center, Bryan, TX, 77807, USA
[b] Department of Psychological & Brain Sciences, Johns Hopkins University, Baltimore, MD, 21218, USA

ARTICLE INFO

Keywords:
Orbitofrontal cortex
Dorsomedial striatum
Synaptic plasticity
Alcohol
Optogenetic
Operant self-administration
Dopamine D1 receptor
Adenosine A2A receptor

ABSTRACT

Uncontrolled drug-seeking and -taking behaviors are generally driven by maladaptive corticostriatal synaptic plasticity. The orbital frontal cortex (OFC) and its projections to the dorsomedial striatum (DMS) have been extensively implicated in drug-seeking and relapse behaviors. The influence of the synaptic plasticity of OFC projections to the DMS (OFC→DMS) on drug-seeking and -taking behaviors has not been fully characterized. To investigate this, we trained rats to self-administer 20% alcohol and then delivered an *in vivo* optogenetic protocol designed to induce long-term potentiation (LTP) selectively at OFC→DMS synapses. We selected LTP induction because we found that voluntary alcohol self-administration suppressed OFC→DMS transmission and LTP may normalize this transmission, consequently reducing alcohol-seeking behavior. Importantly, e*x vivo* slice electrophysiology studies confirmed that this *in vivo* optical stimulation protocol resulted in a significant increase in excitatory OFC→DMS transmission strength on day two after stimulation, suggesting that LTP was induced *in vivo*. Rat alcohol-seeking and -taking behaviors were significantly reduced on days 1–3, but not on days 7–11, after LTP induction. Striatal synaptic plasticity is modulated by several critical neurotransmitter receptors, including dopamine D1 receptors (D1Rs) and adenosine A2A receptors (A2ARs). We found that delivery of *in vivo* optical stimulation in the presence of a D1R antagonist abolished the LTP-associated decrease in alcohol-seeking behavior, whereas delivery in the presence of an A2AR antagonist may facilitate this LTP-induced behavioral change. These results demonstrate that alcohol-seeking behavior was negatively regulated by the potentiation of excitatory OFC→DMS neurotransmission. Our findings provide direct evidence that the OFC exerts "top-down" control of alcohol-seeking behavior via the DMS.

1. Introduction

Drug addiction involves a transition from voluntary use to habitual and inflexible drug-seeking and -taking behaviors (Everitt and Robbins, 2005; Luscher et al., 2020; Volkow et al., 2013). The drug-induced reinforcement of these behaviors is typically driven by maladaptive synaptic plasticity in the corticostriatal pathway (Everitt and Robbins, 2005; Gunaydin and Kreitzer, 2016; Luscher and Malenka, 2011; Luscher et al., 2020; Volkow et al., 2013). Many studies on the control of drug-seeking behavior have focused on subregions of the dorsal striatum and especially on the dorsomedial striatum (DMS) (Gunaydin and Kreitzer, 2016). For instance, previous studies have indicated that repetitive drug use disrupts DMS physiology (Cheng et al., 2017; Everitt and Robbins, 2013; Lu et al., 2019; Wang et al., 2010) and that manipulation of neuronal activity in the DMS can alter alcohol-seeking and -taking behaviors (Cheng et al., 2017; Cheng and Wang, 2019; Hellard et al., 2019; Ma et al., 2018). The DMS receives cortical inputs from many brain regions, including the orbital frontal cortex (OFC) (Bariselli et al., 2020; Hunnicutt et al., 2016; Lu et al., 2021; Smith et al., 2016). Projections from this region to the DMS (OFC→DMS) are strongly linked with inflexible drug-seeking and relapse (Bechara et al., 2001; Burguiere et al., 2015; Micallef and Blin, 2001; Remijnse et al., 2006;

* Corresponding author. 8447 Riverside Pkwy, Suite 2106, Medical Research and Education Building, Bryan, TX, 77807, USA.
E-mail address: jwang188@tamu.edu (J. Wang).

https://doi.org/10.1016/j.neuropharm.2021.108560
Received 16 August 2020; Received in revised form 28 March 2021; Accepted 2 April 2021
Available online 22 April 2021
0028-3908/

Saxena et al., 1998).

Numerous studies in both rodents and humans have demonstrated an executive role of the prefrontal cortex, including the OFC, in decision making and in the top-down control of behaviors (Wright et al., 2008). Hypoactivity of the OFC was identified in alcoholics and other drug users (Alimohamad et al., 2005; Volkow and Fowler, 2000; Volkow et al., 1991), and inhibition of the lateral OFC increased alcohol drinking in alcohol-dependent mice (den Hartog et al., 2016). Furthermore, inhibition of the mammalian target of rapamycin complex 1, which is essential for neuronal plasticity, in the OFC disrupts alcohol relapse and habitual alcohol-seeking behavior (Barak et al., 2013; Morisot et al., 2019). However, the exact mechanism by which synaptic plasticity within the OFC→DMS circuit exerts top-down control of drug-seeking and -taking remains unknown.

In the DMS, dopamine D1 receptors (D1Rs) and adenosine A2A receptors (A2ARs) are critical for striatal plasticity, including long-term potentiation (LTP) and depression (LTD) (Gerfen and Surmeier, 2011; Ma et al., 2018; Shen et al., 2008). Distinct expression of these receptors has been identified within direct-pathway medium spiny neurons (dMSNs) and indirect-pathway MSNs (iMSNs) in the DMS (Augood and Emson, 1994; Gerfen et al., 1990; Oude Ophuis et al., 2014). Previous studies have demonstrated that corticostriatal plasticity in these neurons is critical in the control of alcohol-seeking and -taking behaviors (Bossert et al., 2016; Cheng et al., 2017; Ma et al., 2017, 2018). Both dMSNs and iMSNs in the DMS receive OFC inputs (Lu et al., 2021; Renteria et al., 2018; Wall et al., 2013). Previous research showed that both D1Rs in dMSNs and A2ARs in iMSNs were critically involved in the induction of striatal plasticity (Flajolet et al., 2008; Hellard et al., 2019; Ma et al., 2018; Shen et al., 2008). Thus, the experimental reversal of alcohol-evoked plasticity within the OFC→DMS circuit may provide a deep understanding of how this plasticity controls alcohol-seeking and -taking behaviors.

To achieve this, we trained rats to self-administer 20% alcohol in operant chambers and then delivered our recently developed dual-channel optogenetic LTP-inducing protocol (Ma et al., 2018) to their OFC→DMS synapses. We selected LTP induction because we found that voluntary alcohol self-administration suppressed OFC→DMS transmission and reasoned that LTP normalized this transmission and consequently reduced alcohol-seeking behavior. We found that this *in vivo* induction of OFC→DMS LTP caused a significant reduction in alcohol-seeking and -taking behaviors in the early phase (days 1–3) post-induction; this effect declined over time (days 7–11). This behavioral effect of *in vivo* OFC→DMS LTP was preserved in the presence of an A2AR antagonist (SCH 58261) but was blocked in the presence of a D1R antagonist (SCH 23390). Taken together, the present study has demonstrated a causal link between OFC→DMS synaptic plasticity and alcohol-seeking behavior. This finding supports the proposal that the OFC plays a critical role in top-down control of operant behavior via its projection to the DMS and may provide a novel therapeutic strategy for the treatment of alcohol use disorder.

2. Materials and methods

2.1. Reagents

Adeno-associated virus vector serotype 8 (AAV8)-Syn-Chronos-Green fluorescent protein (GFP) (AAV8-Syn-Chronos-GFP; 5.6×10^{12} vg/mL) and AAV8-Syn-Chrimson-tdTomato (5.5×10^{12} vg/mL) were purchased from the University Of North Carolina Vector Core. SCH 23390 and SCH 58261 were purchased from Tocris. All other reagents were obtained from Sigma.

2.2. Animals

Male Long-Evans rats (3 months old, Harlan Laboratories) were group-housed, with two in each cage. All animals were kept in a temperature- and humidity-controlled environment with a light:dark cycle of 12:12 h (lights on at 7:00 a.m.), with food and water available *ad libitum*. All behavioral experiments were conducted during their light cycle. All animal care and experimental procedures were approved by the Texas A&M University Institutional Animal Care and Use Committee.

2.3. Stereotaxic virus infusion

The stereotaxic viral infusion was performed as described previously (Cheng et al., 2017; Hellard et al., 2019; Huang et al., 2017; Ma et al., 2017, 2018). Viruses were infused into the OFC (AP1: +4.68, ML1: ±1.5 mm, DV1: -4.0 mm; AP2: +4.2, ML2: ±2 mm, DV2: -4.5 mm from Bregma) or the DMS (AP: +1.32 mm, ML: ±2.1 mm, DV: -4.9 mm from Bregma), as indicated. We infused 0.5 μL virus bilaterally into the OFC and 1 μL virus into the DMS at a rate of 0.12 μL/min. At the end of the infusion, the injectors remained in place for 10 min to allow for viral diffusion. Animals were allowed to recover for at least 4 d before they were trained to consume alcohol (Fig. 1A).

2.4. Intermittent access to 20% alcohol two-bottle choice drinking procedure

We employed the intermittent access two-bottle choice drinking procedure, which has been used previously to establish high levels of rat alcohol consumption (Ben Hamida et al., 2013; Cheng et al., 2018; Ehlinger et al., 2017; Hellard et al., 2019; Huang et al., 2017; Lu et al., 2019; Ma et al., 2017, 2018; Wei et al., 2018). Male rats were given 24-h concurrent access to one bottle of 20% alcohol in water (vol/vol) and one bottle of water, starting at 2:00 p.m.; this two-bottle choice was available on alternate days, separated by 24-h periods of access to water only. The water and alcohol bottles were weighed after the 24-h two-bottle choice period unless stated otherwise. This procedure was followed for six weeks.

2.5. Operant self-administration of alcohol

Long-Evans rats were then trained to self-administer a 20% alcohol solution in an operant chamber (Fig. 1A), as previously described (Hellard et al., 2019; Huang et al., 2017; Ma et al., 2018). Each chamber contained an active lever and inactive lever; pressing the active lever resulted in the delivery of an alcohol solution via a dipper, while pressing the inactive lever was recorded but did not result in any alcohol delivery. To shape the magazine entry, rats initially underwent a 30-min training session, where one aliquot (0.1 mL) of 20% alcohol solution was delivered at a random time of 60 s (Bradfield et al., 2013; Corbit et al., 2012). We then shaped our rats to press the lever for alcohol. Briefly, operant sessions were conducted daily in an FR1 schedule so that an active lever press resulted in the delivery of 0.1 mL 20% alcohol. The duration of the training session was gradually shortened from overnight to 1 h. Once rats started to respond more than 10 times in 1 h, an inactive lever was introduced. After the animals' active response rate showed a linear increase for 4 consecutive days, the schedule was then escalated to a random ratio 2 (RR2) schedule for 2 d, followed by an RR3 schedule. Total alcohol consumption was measured for each session, and rats were trained for 5 d a week. The blood alcohol level in rats with a similar training paradigm was reported previously (Ma et al., 2018). Rats that did not reach five rewards in a 1-h FR1 session were excluded for further experiments.

When a stable baseline of active lever pressing was achieved, they underwent surgery for optical fiber implantation (Fig. 1A). RR3 training was resumed one week after the surgery. Once the level of active lever pressing stabilized again, the animals underwent *in vivo* LTP induction. Rats' operant behavior was continuously monitored 11 d after *in vivo* LTP induction. We measured rat active-response rates, alcohol delivery events, normalized alcohol intake, inactive response rates, and latency

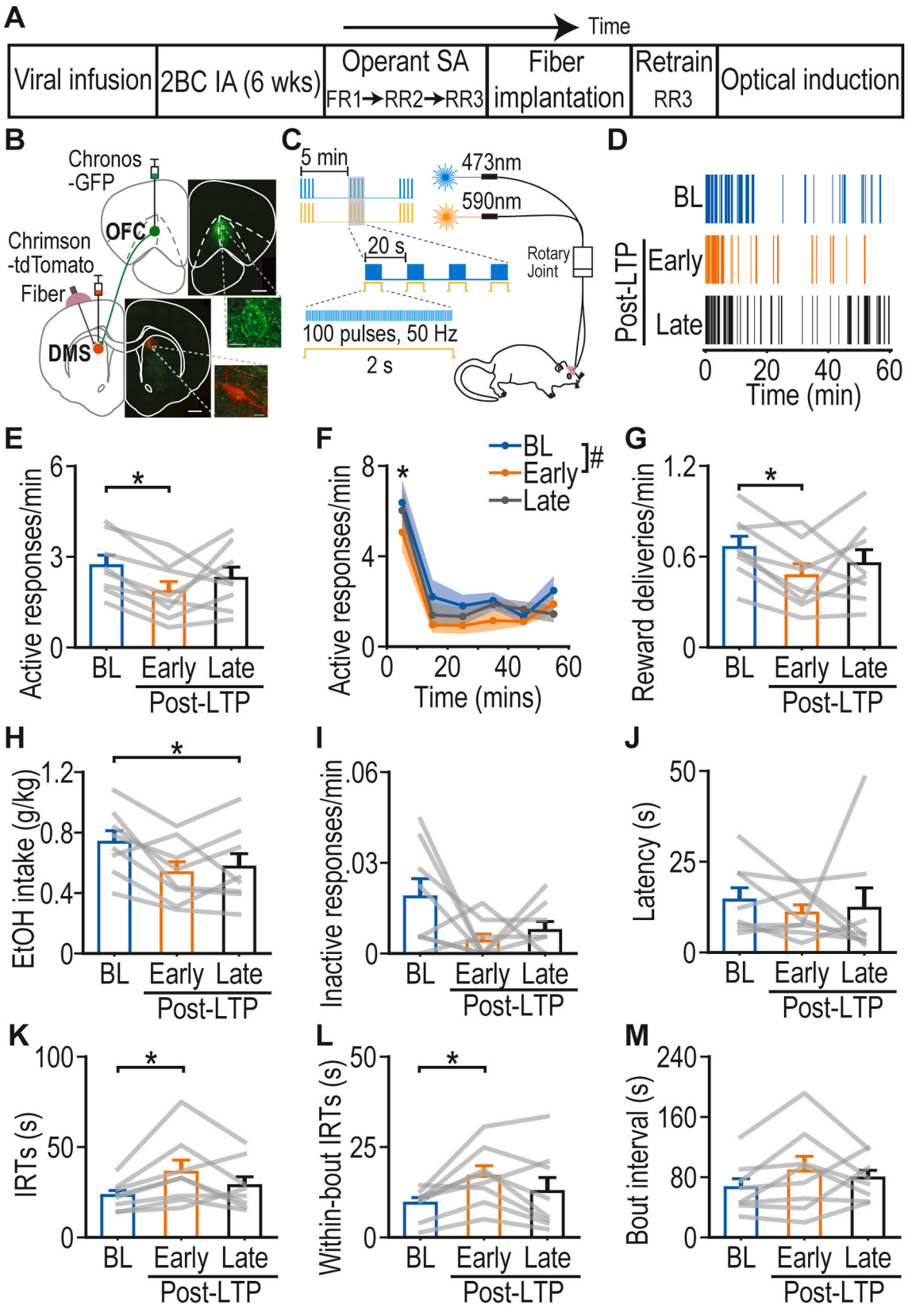

(caption on next page)

Fig. 1. *In vivo* delivery of an optogenetic protocol to induce LTP at OFC→DMS synapses reduced alcohol-seeking behavior during the early phase post-LTP induction. (A) Experimental timeline. All rats underwent viral surgery initially and were then trained to drink 20% alcohol using the two-bottle choice intermittent access procedure (2BC IA) for six weeks (wks). Next, they were trained to perform operant self-administration (SA) of alcohol. The training schedule was gradually increased from fixed ratio 1 (FR1) to random ratio 2 (RR2) and RR3. Following fiber implantation and retraining, LTP was optically induced. (B) Schematic showing viral infusion and optical fiber implantation. AAV8-Syn-Chronos-GFP and AAV8-Syn-Chrimson-tdTomato were infused into the OFC and DMS, as indicated. Optical fibers were implanted into the DMS. Representative confocal images demonstrated Chronos-GFP expression (green) in the OFC (upper), and Chronos-positive fibers (green) and Chrimson-tdTomato expression (red) in DMS neurons (bottom right). Scale bars: 1 mm for the larger lower magnification images and 10 μm for higher magnification images. (C) Schematic of the *in vivo* LTP-inducing protocol. Blue light (473 nm, 2-ms pulses) was delivered at 50 Hz for 2 s; this was paired with a 2-sec constant yellow light (590 nm). This paired stimulation was repeated 4 times at 20-sec intervals. Three such trains of stimulations were repeated at 5-min intervals. (D) Representative timestamps of active lever pressing for alcohol in 60-min sessions conducted at baseline (BL), on days 1–3 post-LTP induction (Early), and on days 7–11 post-LTP induction (Late). (E) A significant decrease in the active response rate for alcohol was observed during the early phase, as compared to BL. Each line represents data from one rat; $^{*}p < 0.05$, one-way RM ANOVA with post hoc SNK test. (F) The time course of the active response rates during the early phase was significantly lower than those during the BL. $\#p < 0.05$, two-way RM ANOVA with post hoc SNK test; $^{*}p < 0.05$ for BL versus Early at the indicated time-point, post hoc SNK test. (G) The alcohol delivery rate was significantly lower during the early phase, as compared to BL; $^{*}p < 0.05$, one-way RM ANOVA with post hoc SNK test. (H) Alcohol (EtOH) intake was significantly lower at both early and late phases post-LTP induction, as compared with BL; $^{*}p < 0.05$, one-way RM ANOVA with post hoc SNK test. (I, J) *In vivo* LTP induction did not alter inactive response rates (I) or the latency before initiation of the first active response in a session (J); $p > 0.05$, one-way RM ANOVA. (K, L) *In vivo* LTP induction increased inter-response times (IRTs) (K) and within-bout IRTs (L) during the early phase, as compared to the BL; $^{*}p < 0.05$, one-way RM ANOVA with post hoc SNK test. (M) *In vivo* LTP induction did not alter the interval between bouts. $p > 0.05$, one-way RM ANOVA. n = 8 rats in D-M.

before initiation of the first active response. To test the effect of SCH 58261 on operant behavior (without LTP induction), we administered saline or 0.5 mg/kg SCH 58261 (Wydra et al., 2015) intraperitoneally (i.p.) on consecutive days, varying the order of administration across the animals (Latin square design). This systemic administration of either SCH 58261 or saline was conducted 30 min before the operant behavior test. After we had completed all essential measurements, we allowed the animal to recover from previous inductions and performed one last LTP induction. The rats were then sacrificed 2 d or 9 d after induction, and electrophysiology recordings were carried out.

2.6. Optical fiber implantation

The fiber implantation was conducted after the acquisition of operant alcohol self-administration (Fig. 1A). Animals were anesthetized with isoflurane and mounted in a stereotaxic frame (Hellard et al., 2019; Ma et al., 2018). An incision was made, and bilateral optical fiber implants (300-nm core fiber secured to a 2.5-mm ceramic ferrule with 5 mm of fiber extending past the end of the ferrule) were lowered into the DMS (AP: +1.32 mm; ML: ±3.0 mm; DV: -4.5 mm from Bregma) at a 10-degree angle. The implants were secured to the skull with metal screws and covered with denture acrylic (Lang Dental). The incision was closed around the head cap. The rats were then monitored for one week or until they resumed regular activity.

2.7. In vivo LTP induction

To induce LTP, paired high-frequency optical stimulation (oHFS) + optical postsynaptic depolarization (oPSD) was delivered via the optical fibers using the following protocol: 100 2-ms pulses of 473-nm light at 50 Hz (oHFS) and a 2-s period of 590-nm light (oPSD), repeated four times at 20-s intervals. This protocol was repeated three times, at 5-min intervals (Ma et al., 2018). This constituted the complete LTP-inducing procedure, which was performed once for each rat in a neutral Plexiglass chamber 30 min before operant testing, with no visual cues. SCH 23390 (0.01 mg/kg) (Ma et al., 2018) or SCH 52816 (0.5 mg/kg) was injected i.p. while the rats were in the home cage, 15 min before LTP induction.

2.8. Preparation of striatal slices and electrophysiology recordings

The slice preparation and whole-cell recording in striatal neurons were conducted as previously described (Cheng et al., 2017, 2018; Hellard et al., 2019; Huang et al., 2017; Lu et al., 2019; Ma et al., 2017, 2018; Wang et al., 2007, 2010, 2011, 2012, 2015; Wei et al., 2018).

Slice preparation. Animals were euthanized, and 250-μm coronal sections containing the DMS were prepared in an ice-cold cutting solution containing (in mM): 40 NaCl, 148.5 sucrose, 4 KCl, 1.25 NaH_2PO_4, 25 $NaHCO_3$, 0.5 $CaCl_2$, 7 $MgCl_2$, 10 glucose, 1 sodium ascorbate, 3 sodium pyruvate, and 3 myoinositol; this solution was saturated with 95% O_2 and 5% CO_2. Slices were then incubated in a 1:1 mixture of the cutting solution and external solution at 32 °C for 45 min. The external solution, which was also saturated with 95% O_2 and 5% CO_2, was composed of the following (in mM): 125 NaCl, 4.5 KCl, 2.5 $CaCl_2$, 1.3 $MgCl_2$, 1.25 NaH_2PO_4, 25 $NaHCO_3$, 15 glucose, and 15 sucrose. Slices were then maintained in the external solution at room temperature until use.

Whole-cell recordings. All recordings were conducted at 32 °C, and slices were perfused with the external solution at a rate of 2–3 mL/min. Picrotoxin (100 μM) was included in the external solution for all recordings in order to block $GABA_A$A receptor-mediated transmission. The pipette solution contained (in mM): 119 $CsMeSO_4$, 8 tetraethylammonium chloride, 15 4-(2-hydroxyethyl) piperazine-1-ethanesulfonic acid (HEPES), 0.6 ethylene glycol tetraacetic acid, 0.3 Na_3GTP, 4 MgATP, 5 QX-314, and 7 phosphocreatine, with an osmolarity of ~280 mOsm/L. The pH was adjusted to 7.3 with CsOH. For selective stimulation of inputs from channelrhodopsin-expressing fibers onto DMS neurons, 473-nm light was delivered through the objective lens for 2 ms. Optically evoked excitatory postsynaptic currents (oEPSCs) were recorded in response to increasing intensities of stimulation. In recordings where Ca^{2+} was replaced with Sr^{2+}, asynchronous EPSC (aEPSC) events were collected from 50 ms after, to 500 ms after each stimulus; the stimuli were delivered once every 30 s in an external solution containing APV (50 μM), 2.5 mM Sr^{2+}, and no Ca^{2+} (Ding et al., 2008; Mateo et al., 2017). Quantal events were analyzed using MiniAnalysis software (Synaptosoft) with detection parameters set at > 5 pA amplitude. For each cell, at least 30 sweeps were taken.

2.9. Statistical analysis

All behavioral data were analyzed using paired *t*-tests, one-way ANOVA with repeated measures (one-way RM ANOVA), or two-way ANOVA with repeated measures (two-way RM ANVOA) followed by Student-Newman-Keuls (SNK) *post hoc* test. Electrophysiological data were analyzed using paired or unpaired *t*-tests and two-way RM ANOVA, followed by the SNK test. We conducted all statistical analyses in OriginLab and SigmaPlot programs. aEPSCs were analyzed using Mini Analysis software (Synaptosoft Inc.). All data are expressed as the mean ± standard error of the mean.

3. Results

3.1. In vivo delivery of an optogenetic LTP-inducing protocol to orbitostriatal synapses within the DMS reduces alcohol-seeking behavior

A recent study found that vapor alcohol exposure decreased glutamatergic OFC→DMS neurotransmission in mice (Renteria et al., 2018). Thus, we reasoned that voluntary alcohol self-administration also decreased this orbitostriatal transmission. A cohort of mice was infused AAV8-Syn-Chronos-GFP in the OFC, trained to consume 20% alcohol using the intermittent access 2-bottle choice drinking procedure for 6 weeks, and trained to self-administer 20% alcohol for another 6 weeks (Supplementary Fig. 1A). DMS slices were prepared 24 h after the last operant session. We found that the oEPSC amplitude was significantly smaller in the alcohol group than in the water controls (Supplementary Fig. 1B; two-way RM ANOVA; $F_{(1,105)} = 39.6$, $p < 0.001$). This result suggests that voluntary alcohol self-administration suppresses OFC→DMS neurotransmission.

The reduced OFC→DMS neurotransmission may, in turn, contribute to operant alcohol self-administration. Next, we examined whether optogenetic strengthening and thus normalizing the OFC→DMS synaptic transmission reduced the operant behavior. To achieve this goal, we infused AAV8-Syn-Chronos-GFP into the OFC and AAV8-Syn-Chrimson-tdTomato into the DMS of Long-Evans rats (Fig. 1A). We selected rats because we found that optogenetic manipulation of DMS synaptic strength in rats altered operant behaviors (Hellard et al., 2019; Ma et al., 2018). The infusion led to Chronos (green) expression in the ventral and lateral OFC, and Chronos-expressing fibers were also observed in the DMS (Fig. 1B). Chrimson-tdTomato expression was exclusively observed in the DMS (Fig. 1B). Then, we trained the virus-infused animals to consume 20% alcohol in the intermittent access two-bottle choice drinking paradigm for six weeks and then self-administered 20% alcohol in operant chambers (Hellard et al., 2019; Huang et al., 2017; Ma et al., 2017, 2018) (Fig. 1A). After a stable operant response was obtained, we implanted optical fibers bilaterally into the DMS (Fig. 1A).

To normalize the alcohol-evoked suppression of OFC→DMS transmission, we delivered an *in vivo* LTP-inducing protocol by pairing oHFS of striatal OFC terminals and oPSD of DMS MSNs in a novel treatment chamber (Ma et al., 2018) (Fig. 1C). We then examined operant alcohol-seeking behavior for 11 d. Based on our previous study (Ma et al., 2018), we divided this time period into an early phase (days 1–3) and a late phase (days 7–11). A decrease in active responses for alcohol was observed in the early post-LTP phase (data were averaged across days 1–3), as compared to baseline (BL) or the late post-LTP phase (data were averaged across days 7–11) (Fig. 1D and E; one-way RM ANOVA; $F_{(2,14)} = 4.23$, $p = 0.037$). Post hoc comparisons revealed a significant difference between BL and the early post-LTP phase ($q = 4.11$, $p = 0.029$), but not between BL and the late post-LTP phase ($q = 2.01$, $p = 0.18$). In contrast, oHFS alone did not alter alcohol-seeking behaviors (Supplementary Fig. 2). Our previous study found that oPSD alone did not alter this operant behavior (Ma et al., 2018). Together, these results suggest that pairing oHFS of the OFC inputs and oPSD of DMS neurons induces a long-lasting suppression of operant alcohol self-administration.

To further investigate how the LTP-inducing protocol affected active responses for the alcohol, we compared this behavior overtime at BL and during the early and late post-LTP phases. Optical induction of LTP at OFC→DMS synapses again significantly reduced the active response rate during the early, but not the late, post-LTP phase, as compared to the BL (Fig. 1F, two-way RM ANOVA; $F_{(2,70)} = 4.23$, $p = 0.037$ for the main effect of the induction; BL versus early phase: $q = 4.11$, $p = 0.029$; BL versus late phase: $q = 2.01$, $p = 0.18$). Consistent with this suppression of active lever pressing for alcohol, the rate of alcohol delivery was also reduced in the early post-LTP phase (Fig. 1G; one-way RM ANOVA; $F_{(2,14)} = 3.63$, $p = 0.05$; BL versus early phase, $q = 3.8$, $p = 0.044$). Next, we examined how *in vivo* optical induction of OFC→DMS LTP affected alcohol-taking behavior. A significant relationship between induction phase and alcohol intake was observed (Fig. 1H; one-way RM ANOVA; $F_{(2,14)} = 6.11$, $p = 0.012$). Interestingly, this behavior was significantly reduced during both early and late post-LTP phases, as compared to BL (early: $q = 4.65$, $p = 0.014$; late: $q = 3.79$, $p = 0.018$). To examine whether OFC→DMS LTP induction caused any deficits in general motor function or attention, we measured the inactive response rate and the latency prior to the first active lever press. There were no significant differences in these measurements after LTP induction, as compared with the BL (Fig. 1I, one-way RM ANOVA, $F_{(2,14)} = 2.34$, $p = 0.13$; Fig. 1J, one-way RM ANOVA, $F_{(2,14)} = 0.24$, $p = 0.79$).

Lastly, we assessed whether the optical induction of OFC→DMS LTP affected the general motor skills in responding to alcohol by analyzing overall inter-response times (IRTs) (Matamales et al., 2017). The IRTs were increased in the early post-LTP phase, as compared to the BL (Fig. 1K; one-way RM ANOVA; $F_{(2,14)} = 5.14$, $p = 0.021$). To further dissociate the motor and motivational effects of this *in vivo* optical stimulation (Brackney et al., 2011; Lu et al., 2019; Yamada and Kanemura, 2020), we performed a response-bout analysis of the active responses. In this analysis, IRTs were categorized into two classes: within-bout IRTs and the interval between bouts. We defined a "bout" period between two lever presses: the first lever press after the last reward collection and the last press that results in a new reward. One-way RM ANOVA reveals that the OFC→DMS LTP induction increased within-bout IRTs (Fig. 1L; one-way RM ANOVA; $F_{(2,14)} = 4.12$, $p = 0.039$), but not alter the interval between response bouts (Fig. 1M; one-way RM ANOVA; $F_{(2,14)} = 1.54$, $p = 0.25$). These data indicate again that the OFC→DMS LTP induction increases the motor control of the seeking behaviors without changing the motivation.

Together, these results suggest that optogenetic delivery of an OFC→DMS LTP-inducing protocol reduced rat alcohol-seeking and -taking behaviors.

3.2. In vivo delivery of an optogenetic LTP-inducing protocol enhances glutamatergic transmission at OFC→DMS synapses

Repeated cycles of alcohol exposure and withdrawals *ex vivo* or *in vivo* facilitate NMDA receptor activity in the dorsal striatum (Ben Hamida et al., 2013; Cheng et al., 2017; Hellard et al., 2019; Ron and Wang, 2009; Wang et al., 2007, 2010, 2011, 2012). This facilitation, in turn, enhances the striatal LTP induction *ex vivo* and *in vivo* (Wang et al., 2012; Ma et al., 2018). To investigate whether the *in vivo* LTP-inducing protocol altered synaptic strength at the OFC→DMS synapse, we recorded DMS neurons in rats exposed to alcohol on day 2 post-LTP induction. The animals were randomly separated into two groups, one with and one without the paired oHFS of striatal OFC terminals and oPSD of DMS MSNs. We first measured 473-nm light-evoked oEPSCs in response to a range of optical stimulation intensities. We found that the plateau oEPSC amplitude was significantly greater in the rats that received the LTP-inducing protocol than those that did not (Fig. 2A; $F_{(1,79)} = 4.45$, $p = 0.048$).

To further investigate this enhancement of OFC→DMS transmission, we used strontium (Sr^{2+}) to replace calcium in the external solution. Sr^{2+}-induced asynchronous responses (aEPSC) have been used previously to investigate synaptic properties (Lu et al., 2019). The OFC terminals were activated by 473-nm light, and aEPSCs were recorded for 500 ms after each stimulus (Fig. 2B). We observed a significantly higher aEPSC frequency in the LTP group than in the control rats (no LTP induction) (Fig. 2C; $t_{(17)} = -2.65$, $p = 0.017$). In addition, the aEPSC amplitude was higher in the LTP group than in control rats (Fig. 2D; $t_{(17)} = -2.50$, $p = 0.023$), indicating that the activity of postsynaptic glutamate receptors was enhanced by *in vivo* LTP induction, i.e., the locus of LTP expression includes at least the postsynaptic site.

To examine whether the enhanced synaptic strength persisted throughout the late post-LTP phase, we trained another two groups of rats and measured oEPSCs and Sr^{2+}-mediated aEPSCs on day 9 after the

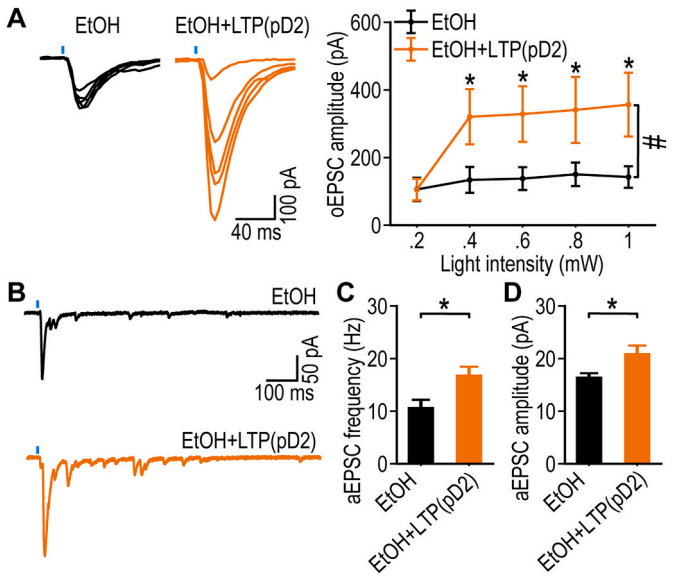

Fig. 2. *In vivo* delivery of the optogenetic LTP-inducing protocol potentiated OFC→DMS synaptic strength in DMS slices prepared during the early post-LTP phase. (A) Left and middle: Sample traces showing potentiation of the optical (473 nm, 2 ms)-evoked excitatory postsynaptic current (oEPSC) on day two after (post day 2, pD2) *in vivo* optical delivery of the OFC→DMS LTP-inducing protocol [EtOH + LTP(pD2)] or after sham LTP induction (EtOH) to alcohol-drinking rats. Right: oEPSC amplitudes generated using the indicated light intensities in rats exposed to EtOH, with and without *in vivo* LTP; $^{\#}p < 0.05$, two-way RM ANOVA; $^{*}p < 0.05$ versus the same light intensity in the EtOH group, post hoc SNK test. n = 11 neurons from 4 rats (EtOH + LTP) and 10 neurons from 4 rats (EtOH). (B) Representative asynchronous EPSC (aEPSC) traces recorded in the presence of Sr^{2+} (2.5 mM) in MSNs from rats exposed to EtOH, with [EtOH + LTP(pD2)] and without (EtOH) *in vivo* LTP induction. (C, D) aEPSC frequency (C) and amplitude (D) increased in rats exposed to EtOH and *in vivo* LTP induction [EtOH + LTP(pD2)], as compared to controls (EtOH); $^{*}p < 0.05$, unpaired *t*-test. n = 10 neurons from 4 rats [EtOH + LTP(pD2)] and 9 neurons from 4 rats (EtOH).

LTP induction. We did not find any significant difference in oEPSC amplitude, aEPSC frequency, or aEPSC amplitude between rats with and without the *in vivo* LTP induction (Supplementary Fig. 3). These data suggest that *in vivo* optogenetically induced LTP did not persist to the late post-LTP phase.

The LTP-inducing protocol includes both oHFS of presynaptic OFC inputs and oPSD of postsynaptic DMS neurons. Our previous study reveals that oPSD alone is insufficient to induce corticostriatal LTP in the DMS (Ma et al., 2018). To test whether oHFS of OFC inputs alone caused long-lasting synaptic changes, we trained another group of rats and measured oEPSCs and Sr^{2+}-mediated aEPSCs 2 days after the *in vivo* oHFS. We did not detect any difference in oEPSC amplitude, aEPSC frequency, or aEPSC amplitude between rats with and without the *in vivo* oHFS (Supplementary Fig. 4). These data suggest that pairing of oHFS and oPSD is required to induce OFC→DMS LTP *in vivo*.

Together, our results demonstrated that *in vivo* delivery of an optogenetic OFC→DMS LTP-inducing protocol, but not oHFS alone, successfully induced synaptic plasticity during the early (day two), but not the late (day nine), post-LTP phase.

3.3. D1R inhibition abolishes the OFC→DMS LTP-mediated reduction in alcohol-seeking behavior

Dopamine signaling is long known to regulate striatal synaptic plasticity (Gerfen and Surmeier, 2011). We and others have previously reported that D1Rs are required for corticostriatal LTP induction in dorsostriatal slices (Ma et al., 2018; Shen et al., 2008). We, therefore, examined whether D1R inhibition during the induction of OFC→DMS LTP altered alcohol-seeking behavior. We administered a D1R antagonist (SCH 23390, 0.01 mg/kg, i.p.) (Cheng et al., 2017; Ma et al., 2018) to the rats 15 min before delivery of paired oHFS terminals and oPSD of DMS MSNs (Fig. 3A). Our previous study found that i.p. injection of SCH 23390 (0.01 mg/kg) alone did not alter operant alcohol self-ministration (Ma et al., 2018). Interestingly, we observed that delivering LTP-inducing protocol in the presence of SCH 23390 caused no significant changes in active response rate during the early or late post-induction phase, as compared with the BL (Fig. 3B and C; one-way RM ANOVA; $F_{(2,14)} = 0.66$, $p = 0.53$). This data suggests that D1R inhibition abolished LTP effects on the operant behavior. To further investigate the effect of D1R inhibition during LTP induction, we examined the active responses overtime after delivery of the LTP-inducing protocol. Two-way RM ANOVA did not reveal any significant effect of the induction, and post hoc comparison failed to detect any significant differences among the BL, the early phase, and the late phase of post-LTP induction (Fig. 3D; two-way RM ANOVA; $F_{(2,70)} = 0.66$, $p = 0.53$ for the main effect of the induction). Consistent with this, no significant differences in alcohol delivery rates (Fig. 3E; one-way RM ANOVA; $F_{(2,14)} = 1.57$, $p = 0.24$) or alcohol intake (Fig. 3F; one-way RM ANOVA; $F_{(2,14)} = 1.48$, $p = 0.26$) between the BL and post-(LTP + SCH 23390). LTP induction in the presence of SCH 23390 did not alter the inactive response rate (Fig. 3G; one-way RM ANOVA; $F_{(2,14)} = 2.36$, $p = 0.13$) or the latency before the first active response to alcohol in each session (Fig. 3H; one-way RM ANOVA; $F_{(2,14)} = 1.18$, $p = 0.34$).

In addition, no statistical difference of IRTs (Fig. 3I; one-way RM ANOVA; $F_{(2,14)} = 0.14$, $p = 0.87$) among the responses during the BL, the early post-LTP phase, and the late post-LTP phases. Interestingly, we found a significant increase in within-bout IRTs during the early phase (Fig. 3J; one-way RM ANOVA; $F_{(2,14)} = 5.31$, $p = 0.019$), as compared to the BL ($q = 3.71$, $p = 0.02$) and the late phase ($q = 4.23$, $p = 0.025$). The interval between response bouts did not differ among three periods (Fig. 3K; one-way RM ANOVA; $F_{(2,14)} = 1.16$, $p = 0.34$).

Collectively, these results indicate that D1R inhibition during LTP induction abolishes the OFC→DMS LTP-mediated reduction in alcohol-seeking and -taking behaviors.

3.4. A2AR inhibition does not block the OFC→DMS LTP-mediated reduction in alcohol-seeking behavior

Given that A2ARs are highly expressed in the striatum (Ballesteros-Yanez et al., 2017; Oude Ophuis et al., 2014) and are also important for striatal LTP induction (Shen et al., 2008), we examined whether inhibition of this receptor changed the OFC→DMS LTP-mediated attenuation of alcohol-seeking behavior.

To address this question, we administered an A2AR antagonist (SCH 58261, 0.5 mg/kg, i.p.) 15 min before the delivery of paired oHFS of striatal OFC terminals and oPSD of DMS MSNs (Fig. 4A). Delivering the LTP protocol in the presence of SCH 58261 significantly affected the active response rate for alcohol (Fig. 4B and C; one-way RM ANOVA, $F_{(2,14)} = 6.45$, $p = 0.01$). Post hoc comparisons detected a significant difference between active response rates during the early phase (days 1–3) post-LTP induction and at BL ($q = 3.53$, $p = 0.026$) or during the late post-LTP phase (days 7–11) ($q = 4.93$, $p = 0.0097$); no significant difference was observed between the active response rate at BL and during the late post-LTP phase ($q = 1.4$, $p = 0.34$). Since the early-phase behavioral consequences of LTP + SCH 58261 (Fig. 4C) and LTP alone (Fig. 1E) seem similar, we performed Hedges' g statistics to compare the effect size of active response reduction in these two experiments (Durlak, 2009; Hedges, 1981). A greater Hedge's g was observed in the LTP + SCH 58261 experiment (Fig. 4C; g = 2.05 for BL versus Early) than in the LTP experiment (Fig. 1E; g = 0.9 for BL versus Early). These results suggest that A2AR inhibition may facilitate LTP induction.

Analysis of the time courses of active responses to alcohol revealed a significant reduction during the early post-induction phase, as compared to the BL and late post-induction phase, in rats treated with SCH 58261

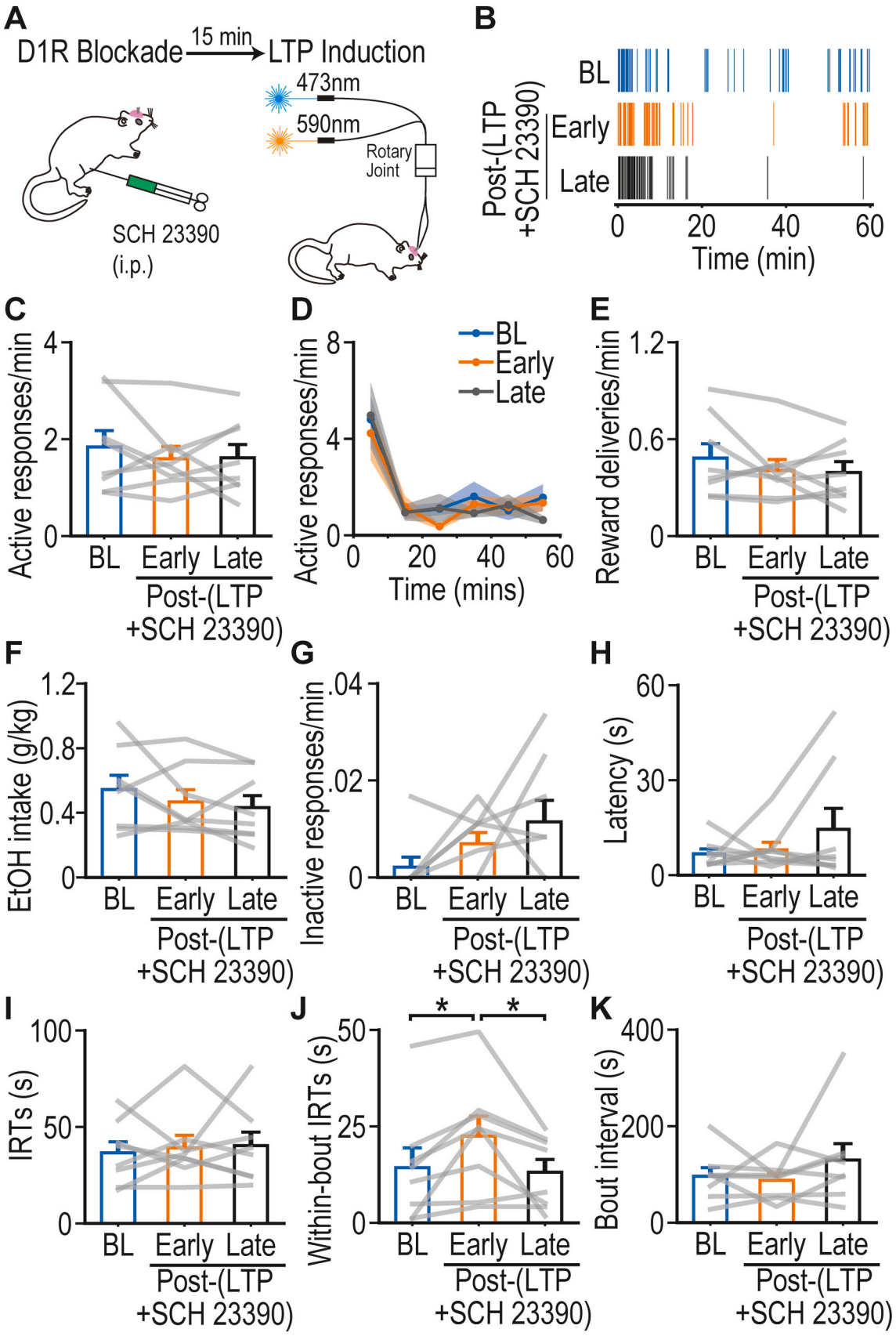

(caption on next page)

Fig. 3. D1R inhibition abolishes the reduction in alcohol-seeking behavior induced by *in vivo* optogenetic OFC→DMS LTP. (A) Schematic showing intraperitoneal (i.p.) administration of the D1 receptor antagonist, SCH 23390 (0.01 mg/kg), 15 min before delivery of the *in vivo* LTP induction protocol (LTP + SCH 23390). (B) Representative timestamps of active lever pressing for alcohol during 60-min sessions conducted at baseline (BL), on days 1–3 post-LTP induction (LTP + SCH 23390) (Early), and on days 7–11 post-LTP induction (Late). (C, D) Active response rates did not differ significantly from BL in the early or late post-induction (LTP + SCH 23390); one-way (C) and two-way (D) RM ANOVA. (E–H) As compared with BL values, *in vivo* LTP induction in the presence of SCH 23390 (LTP + SCH 23390) did not significantly alter the alcohol delivery rate (E), alcohol intake (F), inactive response rate (G), or the latency before initiation of the first active response in a session (H) during the early or late phases post-LTP induction; one-way RM ANOVA. (I–K) *In vivo* LTP induction in the presence of SCH 23390 (LTP + SCH 23390) did not alter the IRTs (I) or bout interval (K) but significantly increased within-bout IRTs (J) in the early post-LTP phase, as compared to BL and the late phase. $P > 0.05$, one-way RM ANOVA for I, K; $^{*}p < 0.05$, one-way RM ANOVA with post hoc SNK test for J. n = 8 rats in C–K.

(Fig. 4D; two-way RM ANOVA; $F_{(2,70)} = 8.12$, $p = 0.0046$ for the main effect of the induction; BL versus. early phase: $q = 4.02$, $p = 0.013$; early versus late phase: $q = 5.51$, $p = 0.0044$). However, there was no difference between the BL and the late phases (Fig. 4D; BL versus. late post-LTP phase, $q = 1.49$, $p = 0.31$) As expected, the alcohol delivery rate was also significantly reduced in rats treated with SCH 58261 prior to induction of LTP; this effect was significant in both the early and late post-LTP phases, as compared to BL (Fig. 4E; one-way RM ANOVA; $F_{(2,14)} = 6.19$, $p = 0.012$). Alcohol intake was also reduced after the induction of LTP in rats treated with SCH 58261 (Fig. 4F; one-way RM ANOVA; $F_{(2,14)} = 4.29$, $p = 0.035$). Although the post hoc comparison only detected a significant recovery of alcohol intake in the late post-LTP phase, as compared to the early post-LTP phase ($q = 3.98$, $p = 0.035$), a paired *t*-test comparison between BL and the early post-LTP phase revealed a significant reduction in alcohol intake ($t_{(7)} = 3.06$, $p = 0.018$). These findings indicated that induction of LTP in rats treated once with this A2AR antagonist reduced alcohol intake. LTP induction in the presence of SCH 58261 did not alter the inactive response rate (Fig. 4G; one-way RM ANOVA; $F_{(2,14)} = 1.65$, $p = 0.23$) or latency before the first active response to alcohol in each session (Fig. 4H; one-way RM ANOVA; $F_{(2,14)} = 0.77$, $p = 0.48$). In addition, we found a significant increase in the active response IRTs during the early post-LTP phase, as compared to the BL and the late phase (Fig. 4I; one-way RM ANOVA; $F_{(2,14)} = 6.64$, $p = 0.0094$). However, we only observed a marginal difference of within-bout IRTs (Fig. 4J; one-way RM ANOVA; $F_{(2,14)} = 3.61$, $p = 0.054$) and bout intervals (Fig. 4K; one-way RM ANOVA; $F_{(2,14)} = 3.21$, $p = 0.071$) among the BL, the early phase, and the late phase.

We then examined whether the dose of SCH 58261 (0.5 mg/kg) used above (Fig. 4) affected alcohol self-administration. To address this question, we retrained the same cohort of rats and administered i.p. SCH 58261 (0.5 mg/kg) or saline on alternate day (Fig. 5A), 30 min before operant self-administration of alcohol. Compared to their performance following saline injection, SCH 58261 administration did not cause any significant change in the rate of active responses for alcohol (Fig. 5B–D; paired *t*-test, $t_{(7)} = 0.68$, $p = 0.52$ for Fig. 5C; one-way RM ANOVA; $F_{(1,35)} = 0.47$, $p = 0.52$ for Fig. 5D). No significant differences in the alcohol delivery rate (Fig. 5E; paired *t*-test, $t_{(7)} = 0.31$, $p = 0.76$), alcohol intake (Fig. 5F; paired *t*-test, $t_{(7)} = -0.74$, $p = 0.48$), inactive responses (Fig. 5G; paired *t*-test, $t_{(7)} = 1.37$, $p = 0.21$), or latency before initiation of the first active response in a session (Fig. 5H; paired *t*-test, $t_{(7)} = -1.16$, $p = 0.28$) were observed in rats treated with SCH 58261 or saline. Lastly, no differences in IRTs (Fig. 5I; paired *t*-test; $t_{(7)} = 0.22$, $p = 0.28$), within-bout IRTs (Fig. 5J; paired *t*-test; $t_{(7)} = -0.94$, $p = 0.28$), or bout intervals (Fig. 5K; paired *t*-test; $t_{(7)} = 0.65$, $p = 0.28$) were observed between the saline and SCH 58261 groups. Taken together, these results indicate that the OFC→DMS LTP-mediated reduction in alcohol-seeking behavior is maintained, may be even facilitated, in rats treated with an A2AR antagonist.

4. Discussion

The present study demonstrates that *in vivo* induction of OFC→DMS LTP reduced alcohol-seeking and -taking behaviors in rats. This effect was apparent during the early post-induction phase (days 1–3) but not during the late post-induction phase (days 7–11). Successful induction of LTP was confirmed in slices obtained 2 d after *in vivo* delivery of the paired oHFS of striatal OFC terminal and oPSD of DMS MSNs. Furthermore, we found that the *in vivo* LTP-induced reductions in alcohol-seeking and -taking behaviors were dependent on the activation of D1Rs and were probably enhanced by inhibition of A2ARs. Our findings suggest that potentiation of OFC→DMS transmission negatively regulates alcohol-seeking behavior. These findings support the idea that the OFC, at least in part, mediates "top-down" control via its projections to the DMS.

Loss of control over alcohol drinking represents a hallmark of alcohol use disorder (Barker and Taylor, 2014; Corbit and Janak, 2016; Everitt and Robbins, 2005). Although previous studies have identified an inhibitory role of the OFC in the regulation of alcohol-seeking and -taking (Barak et al., 2013; den Hartog et al., 2016; Morisot et al., 2019), we discovered that chronic voluntary alcohol self-administration suppressed OFC→DMS synaptic transmission in the rodent. This is consistent with the recent finding that chronic alcohol vapor exposure disrupts the glutamate transmission from OFC terminals onto the DMS neurons (Renteria et al., 2018). Thus, our study provides further evidence supporting the concept that chronic alcohol exposure, regardless of exposure routes, suppresses the synaptic strength between the OFC and the DMS.

The present study found that delivering an *in vivo* LTP inducing protocol to OFC→DMS synapses caused a long-lasting (at least three days) reduction of alcohol-seeking and -taking behavior, which persists longer than those generated by many previously reported pharmacological or chemogenetic interventions (Cheng et al., 2017; den Hartog et al., 2016; Wang et al., 2015). The LTP-inducing protocol employs oHFS of presynaptic OFC inputs and oPSD of postsynaptic striatal neurons. Our previous study found that oPSD alone did not cause long-term synaptic plasticity in the striatum (Ma et al., 2018). In this study, we confirmed that oHFS alone did not change alcohol-seeking behaviors. Although an HFS protocol was reported to induce corticostriatal LTD in brain slices (Gerdeman et al., 2002) and in anesthetized or awake rats (Bariselli et al., 2020; Reynolds and Wickens, 2000), the HFS-induced LTD was only examined less than 24 h after the induction. We provided further evidence that the HFS alone is insufficient to drive a long-lasting (e.g., 1 d) change in corticostriatal synaptic strength. Therefore, an optogenetic protocol that can *in vivo* manipulate both pre- and postsynaptic activity is likely to cause more robust and persistent behavioral changes than those protocols that merely manipulate presynaptic activity.

The LTP-inducing protocol employed in the present study was previously used to potentiate medial prefrontal cortex (mPFC)→DMS synapses. Although both the mPFC and OFC send glutamatergic projections to the DMS, the present study found that OFC→DMS LTP produced the opposite effect on behavior, as compared with our previous findings relating to mPFC→DMS plasticity (Ma et al., 2018). There could be two potential reasons for this difference. Even though both the prefrontostriatal and orbitostriatal pathways are essential for flexible goal-directed behavior (Balleine et al., 2015), several studies have indicated that the mPFC and OFC encode different decision-making information relating to behavioral flexibility (Churchwell et al., 2010; Rudebeck et al., 2006; Young and Shapiro, 2009). Thus, manipulation of the plasticity of these pathways may produce a distinct effect on decision processing, and further studies are required to characterize these effects. The second potential reason for the difference observed is that the LTP-inducing

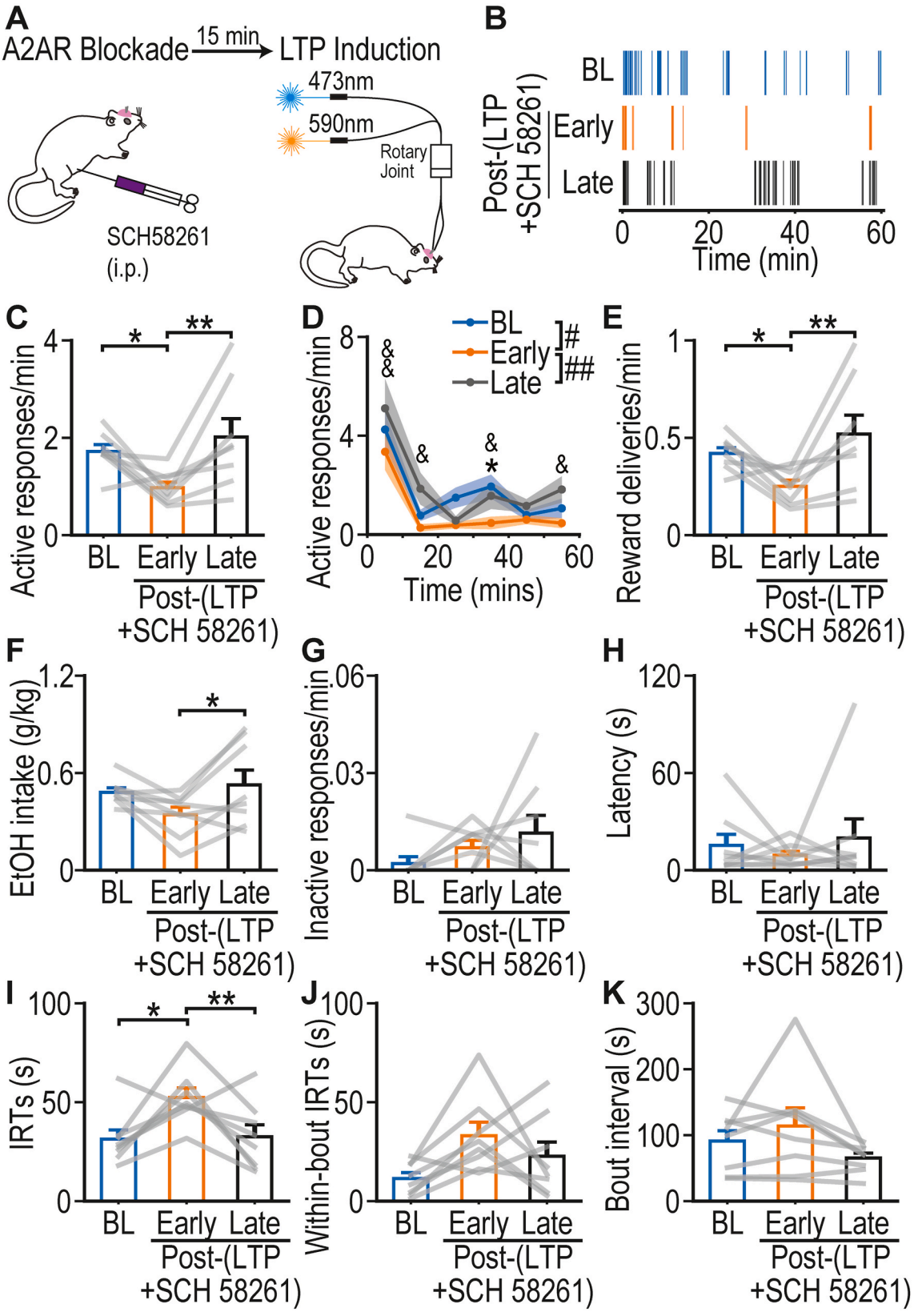

(caption on next page)

Fig. 4. *In vivo* optogenetic induction of OFC→DMS LTP in the presence of an A2AR antagonist resulted in a reduction in alcohol-seeking behavior during the early phase post-LTP induction. (A) Schematic showing i.p. administration of the A2A receptor antagonist, SCH 58261 (0.5 mg/kg), 15 min before delivery of the *in vivo* LTP-inducing protocol (LTP + SCH 58261). (B) Representative timestamps of active lever pressing for alcohol during 60-min sessions conducted at baseline (BL), on days 1–3 post-induction (LTP + SCH 58261) (Early), and on days 7–11 post-induction (Late). (C) Active response rates were significantly lower during the early phase post-induction (LTP + SCH 58261), as compared to BL or the late phase; $^{*}p < 0.05$, $^{**}p < 0.01$, one-way RM ANOVA with post hoc SNK test. (D) The time course of the active responses rates in the presence of SCH5 8261 (LTP + SCH 58261) during the early phase post-LTP induction was significantly lower than those from the BL and late phase. $^{\#}p < 0.05$, $^{\#\#}p < 0.01$ for comparison between the induction phases, two-way RM ANOVA with post hoc SNK test; $^{*}p < 0.05$ for BL versus Early at the indicated time point, post hoc SNK test; $^{\&}p < 0.05$, $^{\&\&}p < 0.01$ for Early versus Late at the indicated time point, post hoc SNK test. (E) The alcohol delivery rate was significantly lower in the early phase post-induction (LTP + SCH 58261), as compared to the BL or late phase; $^{*}p < 0.05$, $^{**}p < 0.01$, one-way RM ANOVA with post hoc SNK test. (F) Alcohol intake was significantly lower in the early phase than in the late phase induction (LTP + SCH 58261); $^{*}p < 0.05$, one-way RM ANOVA with post hoc SNK test. (G, H) *In vivo* LTP induction in the presence of SCH 58261 did not alter the inactive response rate (G) or the latency before initiation of the first active response of a session (H); $p > 0.05$, one-way RM ANOVA. (I) *In vivo* LTP induction in the presence of SCH (LTP + SCH 58261) significantly increased the IRTs in the early phase, as compared to the BL and the late phase; $^{*}p < 0.05$, $^{**}p < 0.01$, one-way RM ANOVA with post hoc SNK test. (J, K) The induction (LTP + SCH 58261) did not significantly change within-bout IRTs (J) or bout interval (K) crossing each induction phase (BL, Early, and Late), $p > 0.05$, one-way RM ANOVA. n = 8 rats in C–K.

protocol employed in the present study may therefore have counteracted the alcohol-induced disruption of OFC→DMS synapses. No difference in the inactive response and initial active response latency suggests that *in vivo* LTP induction is unlikely to produce general attention and motor function deficits. However, we still found alterations of general IRTs and within-bout IRTs during the early post-LTP phase. These alterations indicate that OFC→DMS transmission controls some aspect of motor skills or motor activity (Bariselli et al., 2020; Matamales et al., 2017; Wall et al., 2019).

Next, we confirmed that *in vivo* delivery of the OFC→DMS LTP-inducing protocol enhanced the amplitude of oEPSC recorded 2 d after LTP induction. This indicated a potentiation of OFC→DMS synaptic strength. This evidence is consistent with our previous study, where the same protocol produced a robust LTP at mPFC→DMS synapses (Ma et al., 2018). Different shapes of oEPSC input-output curves found in several experiments may result from the different species, animals, and batches of viruses used. The reasons why lower intensities of light stimulation were required in mouse slices than in rat slices are not known. It has been reported that neuronal densities of the whole brain and of the cortex are higher in mice than in rats (Herculano-Houzel et al., 2006; Keller et al., 2018; Ren et al., 1992). Thus, the density of the OFC inputs within the DMS is likely to be higher in mice than in rats. When a similar amount of virus was infused into rat and mouse striatum, the same light stimulation may activate more OFC inputs in mouse slices than in rat slices, which may lead to that less light intensities are needed. Importantly, in addition to enhancing the oEPSC amplitude, the present study found that *in vivo* LTP induction also increased the frequency and amplitude of aEPSCs. An increase in aEPSC amplitude suggests an enhancement of presynaptic vesicle size or of the postsynaptic AMPAR-mediated current (Sciamanna et al., 2015), an increase in aEPSC frequency indicates an increased probability of glutamate release from OFC terminals (Mateo et al., 2017; Renteria et al., 2018). More importantly, we further confirmed that the synaptic strengthening elicited by the *in vivo* LTP-inducing protocol did not persist in the late post-LTP phase, at which time point we observed a recovery of alcohol-seeking behaviors back to the basal level. Together with the examination of synaptic strength at day two post-LTP induction, these results imply that strengthening OFC→DMS neurotransmission is sufficient and necessary to reduce alcohol-seeking behaviors.

The application of the LTP-inducing protocol at OFC→DMS synapses in the present study may potentiate the synaptic strength of OFC projections to both dMSNs and iMSNs (Ma et al., 2018). Given that dMSNs and iMSNs exert opposite influences on alcohol-taking behavior (Cheng et al., 2017), the observed effects of *in vivo* optogenetic OFC→DMS LTP induction on alcohol-seeking and -taking behaviors may involve both dMSNs and iMSNs, which almost exclusively express D1Rs and A2ARs in the rat striatum, respectively (Kreitzer and Malenka, 2008; Oude Ophuis et al., 2014). In this study, we showed that D1R inhibition during *in vivo* OFC→DMS LTP induction prevented the LTP-induced reduction in alcohol-seeking behaviors. Previous publications have suggested that D1Rs are essential for corticostriatal LTP induction (Cahill et al., 2014; Kerr and Wickens, 2001). Therefore, D1R inhibition while delivering LTP-inducing protocol probably abolishes LTP-induction on dMSNs, but not on iMSNs (Centonze et al., 2003; Lovinger et al., 2003; Ma et al., 2018; Shen et al., 2008). This data implies that strengthening OFC→dMSN transmission may play an essential role in controlling alcohol-seeking and -taking behaviors. Although induction of OFC→DMS LTP did not alter the active alcohol-seeking response rate, the within-bout response rate did slowdown in the early post-LTP phase. This is probably because iMSN activation increases the control of motor function (Bateup et al., 2010; Kravitz et al., 2012).

In contrast, the A2AR is critical for the induction of LTP at iMSNs in the DMS (Flajolet et al., 2008; Shen et al., 2008). Administration of the A2AR antagonist prior to delivery of the *in vivo* optogenetic LTP protocol was therefore likely to prevent LTP at iMSNs while preserving LTP at dMSNs. The effect of A2AR inhibition on LTP-induced reduction of active response rates was evidenced by a greater effect size in the LTP + SCH 58261 group than in the LTP group. These results indicate again that OFC→DMS dMSNs connection is more important than OFC→DMS iMSNs in controlling alcohol-seeking behavior, which is supported by the fact that chronic vapor alcohol exposure selectively disrupts OFC transmission in DMS dMSNs (Renteria et al., 2018). Therefore, inducing OFC→DMS LTP in the presence of D1R activity and A2AR blockade may provide a therapeutic strategy capable of inducing a sustained reduction in alcohol-seeking behavior. Although optogenetic treatment is not currently an option in alcohol use disorder, repetitive transcranial magnetic stimulation (rTMS) (Huang et al., 2005) or deep brain stimulation (Creed et al., 2015) are available for use in humans and are able to induce LTP *in vivo*. We believe that combined use of rTMS and deep brain stimulation, together with a D1R agonist and an A2AR antagonist, may provide a novel clinical treatment for alcohol use disorder.

In summary, our results have demonstrated that optogenetic induction of LTP at OFC→DMS synapses reduced alcohol-seeking and -taking behaviors in rats. This finding suggests that OFC→DMS synaptic plasticity plays a crucial role in the "top-down" control of alcohol-seeking behavior. Furthermore, we show that OFC→DMS plasticity-mediated control of alcohol-seeking behavior is D1R-dependent. Importantly, the LTP-associated reduction in alcohol-seeking behavior was enhanced in the presence of an A2AR antagonist. Our research establishes a direct link between OFC→DMS synaptic potentiation and "top-down" control of alcohol-seeking behavior and provides insights to inform potential therapeutic strategies aimed at reducing alcohol-seeking and relapse.

Data availability

The datasets generated for this manuscript are available on request to jwang188@tamu.edu.

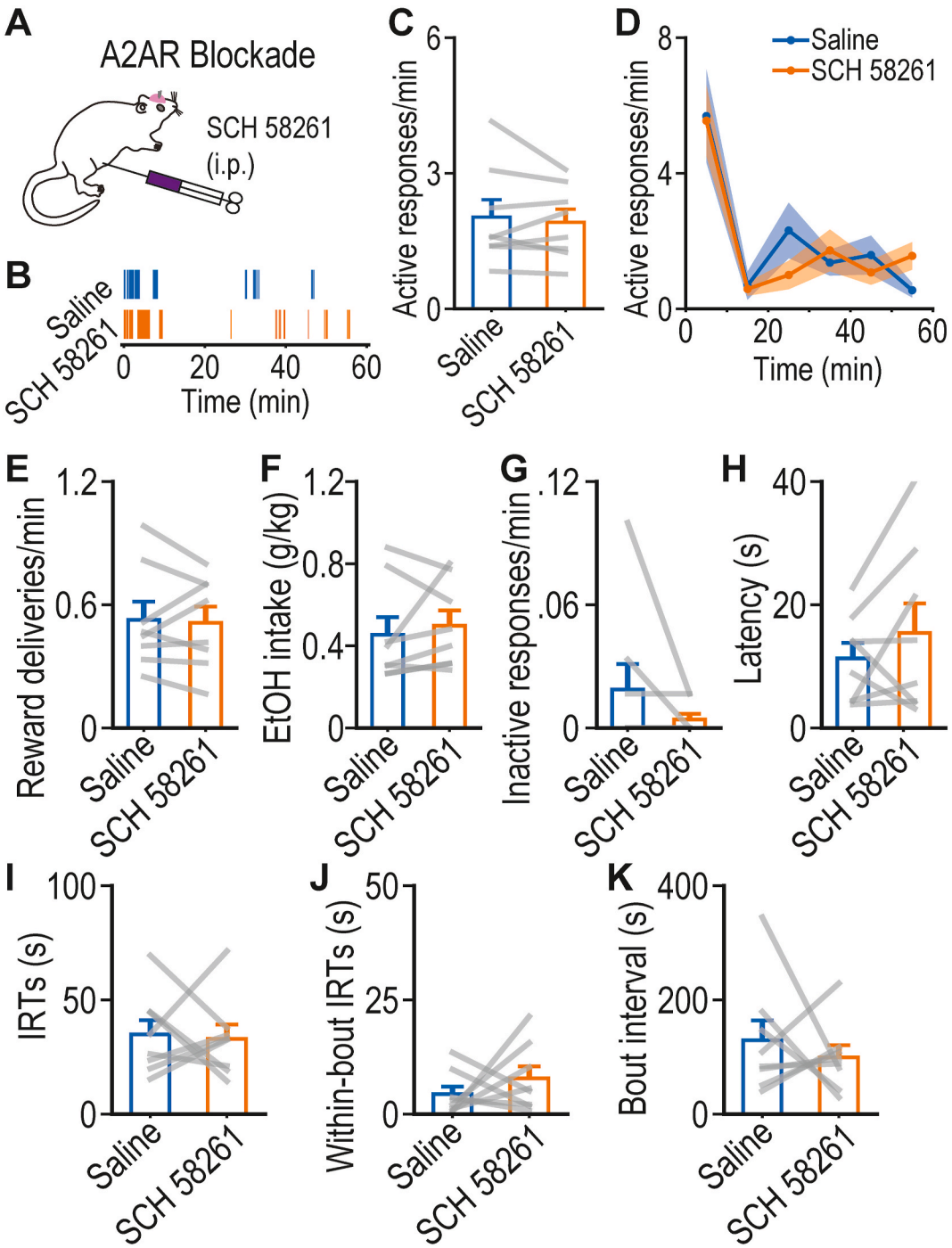

Fig. 5. A2AR inhibition alone did not alter alcohol-seeking behavior. (A) Schematic showing i.p. administration of the A2AR receptor antagonist, SCH 58261, or saline. (B) Representative timestamps of active responses for alcohol by rats treated with i.p. saline or i.p. SCH 58261 (0.5 mg/kg). (C, D) Systemic administration of SCH 58261 did not change the averaged (C) or time courses (D) of the active response rate; $p > 0.05$, paired *t*-test for C; two-way RM ANOVA for D. (E–K) Systemic administration of SCH 58261 did not change the alcohol delivery rate (E), alcohol intake (F), inactive response rate (G), latency before initiation of the first active response in a session (H), the IRTs (I), within-bout IRTs (J), or bout interval (K), as compared to saline injection (BL); $p > 0.05$, paired *t*-test. n = 8 rats in C–K.

Ethics statement

All animal care and experimental procedures were approved by the Texas A&M University Institutional Animal Care and Use Committee and were conducted in accordance with the *National Research Council Guide for the Care and Use of Laboratory Animals*.

Author contributions

JW and PJ conceived of, designed, and supervised all experiments in the study. JW and YC wrote and revised the manuscript. YC designed all behavior experiments, conducted major optical stimulations and systemic drug administration, and analyzed the behavioral data. XX conducted behavioral experiments and conducted the rest optical stimulations. JL, HG, WW designed and performed all electrophysiology experiments and analyzed the data. SM, XW, JJ, KW and YH help with

behavioral experiments. EG designed IRT analysis for all behavioral data. All authors discussed the results and commented on the manuscript.

Funding

This research was supported by NIAAA R01AA021505 (JW), R01AA027768 (JW), U01AA025932 (JW), R01AA026306 (PJ), NIDA R01DA035943 (PJ), and an X-Grant from the Presidential Excellence Fund at Texas A&M University (JW).

Declaration of competing interest

None.

Appendix A. Supplementary data

Supplementary data to this article can be found online at https://doi.org/10.1016/j.neuropharm.2021.108560.

References

Alimohamad, H., Rajakumar, N., Seah, Y.H., Rushlow, W., 2005. Antipsychotics alter the protein expression levels of beta-catenin and GSK-3 in the rat medial prefrontal cortex and striatum. Biol. Psychiatr. 57, 533–542.
Augood, S.J., Emson, P.C., 1994. Adenosine A2a receptor mRNA is expressed by enkephalin cells but not by somatostatin cells in rat striatum: a co-expression study. Brain Res. Mol. Brain Res. 22, 204–210.
Balleine, B.W., Dezfouli, A., Ito, M., Doya, K., 2015. Hierarchical control of goal-directed action in the cortical–basal ganglia network. Curr. Opin. Behav. Sci. 5, 1–7.
Ballesteros-Yanez, I., Castillo, C.A., Merighi, S., Gessi, S., 2017. The role of adenosine receptors in psychostimulant addiction. Front. Pharmacol. 8, 985.
Barak, S., Liu, F., Ben Hamida, S., Yowell, Q.V., Neasta, J., Kharazia, V., Janak, P.H., Ron, D., 2013. Disruption of alcohol-related memories by mTORC1 inhibition prevents relapse. Nat. Neurosci. 16, 1111–1117.
Bariselli, S., Miyazaki, N.L., Creed, M.C., Kravitz, A.V., 2020. Orbitofrontal-striatal potentiation underlies cocaine-induced hyperactivity. Nat. Commun. 11, 3996.
Barker, J.M., Taylor, J.R., 2014. Habitual alcohol seeking: modeling the transition from casual drinking to addiction. Neurosci. Biobehav. Rev. 47, 281–294.
Bateup, H.S., Santini, E., Shen, W., Birnbaum, S., Valjent, E., Surmeier, D.J., Fisone, G., Nestler, E.J., Greengard, P., 2010. Distinct subclasses of medium spiny neurons differentially regulate striatal motor behaviors. Proc. Natl. Acad. Sci. U. S. A. 107, 14845–14850.
Bechara, A., Dolan, S., Denburg, N., Hindes, A., Anderson, S.W., Nathan, P.E., 2001. Decision-making deficits, linked to a dysfunctional ventromedial prefrontal cortex, revealed in alcohol and stimulant abusers. Neuropsychologia 39, 376–389.
Ben Hamida, S., Darcq, E., Wang, J., Wu, S., Phamluong, K., Kharazia, V., Ron, D., 2013. Protein tyrosine phosphatase alpha in the dorsomedial striatum promotes excessive ethanol-drinking behaviors. J. Neurosci. 33, 14369–14378.
Bossert, J.M., Adhikary, S., St Laurent, R., Marchant, N.J., Wang, H.L., Morales, M., Shaham, Y., 2016. Role of projections from ventral subiculum to nucleus accumbens shell in context-induced reinstatement of heroin seeking in rats. Psychopharmacology (Berlin) 233, 1991–2004.
Brackney, R.J., Cheung, T.H., Neisewander, J.L., Sanabria, F., 2011. The isolation of motivational, motoric, and schedule effects on operant performance: a modeling approach. J. Exp. Anal. Behav. 96, 17–38.
Bradfield, L.A., Bertran-Gonzalez, J., Chieng, B., Balleine, B.W., 2013. The thalamostriatal pathway and cholinergic control of goal-directed action: interlacing new with existing learning in the striatum. Neuron 79, 153–166.
Burguiere, E., Monteiro, P., Mallet, L., Feng, G., Graybiel, A.M., 2015. Striatal circuits, habits, and implications for obsessive–compulsive disorder. Curr. Opin. Neurobiol. 30, 59–65.
Cahill, E., Pascoli, V., Trifilieff, P., Savoldi, D., Kappes, V., Luscher, C., Caboche, J., Vanhoutte, P., 2014. D1R/GluN1 complexes in the striatum integrate dopamine and glutamate signalling to control synaptic plasticity and cocaine-induced responses. Mol. Psychiatr. 19, 1295–1304.
Centonze, D., Grande, C., Saulle, E., Martin, A.B., Gubellini, P., Pavon, N., Pisani, A., Bernardi, G., Moratalla, R., Calabresi, P., 2003. Distinct roles of D1 and D5 dopamine receptors in motor activity and striatal synaptic plasticity. J. Neurosci. 23, 8506–8512.
Cheng, Y., Huang, C.C.Y., Ma, T., Wei, X., Wang, X., Lu, J., Wang, J., 2017. Distinct synaptic strengthening of the striatal direct and indirect pathways drives alcohol consumption. Biol. Psychiatr. 81, 918–929.
Cheng, Y., Wang, J., 2019. The use of chemogenetic approaches in alcohol use disorder research and treatment. Alcohol 74, 39–45.
Cheng, Y., Wang, X., Wei, X., Xie, X., Melo, S., Miranda, R.C., Wang, J., 2018. Prenatal exposure to alcohol induces functional and structural plasticity in dopamine D1 receptor-expressing neurons of the dorsomedial striatum. Alcohol Clin. Exp. Res. 42, 1493–1502.
Churchwell, J.C., Morris, A.M., Musso, N.D., Kesner, R.P., 2010. Prefrontal and hippocampal contributions to encoding and retrieval of spatial memory. Neurobiol. Learn. Mem. 93, 415–421.
Corbit, L.H., Janak, P.H., 2016. Habitual alcohol seeking: neural bases and possible relations to alcohol use disorders. Alcohol Clin. Exp. Res. 40, 1380–1389.
Corbit, L.H., Nie, H., Janak, P.H., 2012. Habitual alcohol seeking: time course and the contribution of subregions of the dorsal striatum. Biol. Psychiatr. 72, 389–395.
Creed, M., Pascoli, V.J., Luscher, C., 2015. Addiction therapy. Refining deep brain stimulation to emulate optogenetic treatment of synaptic pathology. Science 347, 659–664.
den Hartog, C., Zamudio-Bulcock, P., Nimitvilai, S., Gilstrap, M., Eaton, B., Fedarovich, H., Motts, A., Woodward, J.J., 2016. Inactivation of the lateral orbitofrontal cortex increases drinking in ethanol-dependent but not non-dependent mice. Neuropharmacology 107, 451–459.
Ding, J., Peterson, J.D., Surmeier, D.J., 2008. Corticostriatal and thalamostriatal synapses have distinctive properties. J. Neurosci. 28, 6483–6492.
Durlak, J.A., 2009. How to select, calculate, and interpret effect sizes. J. Pediatr. Psychol. 34, 917–928.
Ehlinger, D.G., Burke, J.C., McDonald, C.G., Smith, R.F., Bergstrom, H.C., 2017. Nicotine-induced and D1-receptor-dependent dendritic remodeling in a subset of dorsolateral striatum medium spiny neurons. Neuroscience 356, 242–254.
Everitt, B.J., Robbins, T.W., 2005. Neural systems of reinforcement for drug addiction: from actions to habits to compulsion. Nat. Neurosci. 8, 1481–1489.
Everitt, B.J., Robbins, T.W., 2013. From the ventral to the dorsal striatum: devolving views of their roles in drug addiction. Neurosci. Biobehav. Rev. 37, 1946–1954.
Flajolet, M., Wang, Z., Futter, M., Shen, W., Nuangchamnong, N., Bendor, J., Wallach, I., Nairn, A.C., Surmeier, D.J., Greengard, P., 2008. FGF acts as a co-transmitter through adenosine A(2A) receptor to regulate synaptic plasticity. Nat. Neurosci. 11, 1402–1409.
Gerdeman, G.L., Ronesi, J., Lovinger, D.M., 2002. Postsynaptic endocannabinoid release is critical to long-term depression in the striatum. Nat. Neurosci. 5, 446–451.
Gerfen, C.R., Engber, T.M., Mahan, L.C., Susel, Z., Chase, T.N., Monsma Jr., F.J., Sibley, D.R., 1990. D1 and D2 dopamine receptor-regulated gene expression of striatonigral and striatopallidal neurons. Science 250, 1429–1432.
Gerfen, C.R., Surmeier, D.J., 2011. Modulation of striatal projection systems by dopamine. Annu. Rev. Neurosci. 34, 441–466.
Gunaydin, L.A., Kreitzer, A.C., 2016. Cortico-basal ganglia circuit function in psychiatric disease. Annu. Rev. Physiol. 78, 327–350.
Hedges, L.V., 1981. Distribution theory for glass's estimator of effect size and related estimators. J. Educ. Stat. 6, 107–128.
Hellard, E.R., Binette, A., Zhuang, X., Lu, J., Ma, T., Jones, B., Williams, E., Jayavelu, S., Wang, J., 2019. Optogenetic control of alcohol-seeking behavior via the dorsomedial striatal circuit. Neuropharmacology 155, 89–97.
Herculano-Houzel, S., Mota, B., Lent, R., 2006. Cellular scaling rules for rodent brains. Proc. Natl. Acad. Sci. U. S. A. 103, 12138–12143.
Huang, C.C., Ma, T., Hellard, E.A.R., Wang, X., Selvamani, A., Lu, J., Sohrabji, F., Wang, J., 2017. Stroke triggers nigrostriatal plasticity and increases alcohol consumption in rats. Sci. Rep. 7, 2501.
Huang, Y.Z., Edwards, M.J., Rounis, E., Bhatia, K.P., Rothwell, J.C., 2005. Theta burst stimulation of the human motor cortex. Neuron 45, 201–206.
Hunnicutt, B.J., Jongbloets, B.C., Birdsong, W.T., Gertz, K.J., Zhong, H., Mao, T., 2016. A comprehensive excitatory input map of the striatum reveals novel functional organization. Elife 5, e19103.
Keller, D., Ero, C., Markram, H., 2018. Cell densities in the mouse brain: a systematic review. Front. Neuroanat. 12, 83.
Kerr, J.N.D., Wickens, J.R., 2001. Dopamine D-1/D-5 receptor activation is required for long-term potentiation in the rat neostriatum in vitro. J. Neurophysiol. 85, 117–124.
Kravitz, A.V., Tye, L.D., Kreitzer, A.C., 2012. Distinct roles for direct and indirect pathway striatal neurons in reinforcement. Nat. Neurosci. 15, 816–818.
Kreitzer, A.C., Malenka, R.C., 2008. Striatal plasticity and basal ganglia circuit function. Neuron 60, 543–554.
Lovinger, D.M., Partridge, J.G., Tang, K.C., 2003. Plastic control of striatal glutamatergic transmission by ensemble actions of several neurotransmitters and targets for drugs of abuse. Ann. N. Y. Acad. Sci. 1003, 226–240.
Lu, J., Cheng, Y., Wang, X., Woodson, K., Kemper, C., Disney, E., Wang, J., 2019. Alcohol intake enhances glutamatergic transmission from D2 receptor-expressing afferents onto D1 receptor-expressing medium spiny neurons in the dorsomedial striatum. Neuropsychopharmacology 44, 1123–1131.
Lu, J., Cheng, Y., Xie, X., Woodson, K., Bonifacio, J., Disney, E., Barbee, B., Wang, X., Zaidi, M., Wang, J., 2021. Whole-brain mapping of direct inputs to dopamine D1 and D2 receptor-expressing medium spiny neurons in the posterior dorsomedial striatum. eNeuro 8.
Luscher, C., Malenka, R.C., 2011. Drug-evoked synaptic plasticity in addiction: from molecular changes to circuit remodeling. Neuron 69, 650–663.
Luscher, C., Robbins, T.W., Everitt, B.J., 2020. The transition to compulsion in addiction. Nat. Rev. Neurosci. 21, 247–263.
Ma, T., Barbee, B., Wang, X., Wang, J., 2017. Alcohol induces input-specific aberrant synaptic plasticity in the rat dorsomedial striatum. Neuropharmacology 123, 46–54.
Ma, T., Cheng, Y., Roltsch Hellard, E., Wang, X., Lu, J., Gao, X., Huang, C.C.Y., Wei, X., Ji, J., Wang, J., 2018. Bidirectional and long-lasting control of alcohol-seeking behavior by corticostriatal LTP and LTD. Nat. Neurosci. 21, 373–383.
Matamales, M., Skrbis, Z., Bailey, M.R., Balsam, P.D., Balleine, B.W., Gotz, J., Bertran-Gonzalez, J., 2017. A corticostriatal deficit promotes temporal distortion of automatic action in ageing. Elife 6.
Mateo, Y., Johnson, K.A., Covey, D.P., Atwood, B.K., Wang, H.L., Zhang, S., Gildish, I., Cachope, R., Bellocchio, L., Guzman, M., Morales, M., Cheer, J.F., Lovinger, D.M.,

2017. Endocannabinoid actions on cortical terminals orchestrate local modulation of dopamine release in the nucleus accumbens. Neuron 96, 1112–1126 e1115.
Micallef, J., Blin, O., 2001. Neurobiology and clinical pharmacology of obsessive-compulsive disorder. Clin. Neuropharmacol. 24, 191–207.
Morisot, N., Phamluong, K., Ehinger, Y., Berger, A.L., Moffat, J.J., Ron, D., 2019. mTORC1 in the orbitofrontal cortex promotes habitual alcohol seeking. Elife 8.
Oude Ophuis, R.J., Boender, A.J., van Rozen, A.J., Adan, R.A., 2014. Cannabinoid, melanocortin and opioid receptor expression on DRD1 and DRD2 subpopulations in rat striatum. Front. Neuroanat. 8, 14.
Remijnse, P.L., Nielen, M.M., van Balkom, A.J., Cath, D.C., van Oppen, P., Uylings, H.B., Veltman, D.J., 2006. Reduced orbitofrontal-striatal activity on a reversal learning task in obsessive-compulsive disorder. Arch. Gen. Psychiatr. 63, 1225–1236.
Ren, J.Q., Aika, Y., Heizmann, C.W., Kosaka, T., 1992. Quantitative analysis of neurons and glial cells in the rat somatosensory cortex, with special reference to GABAergic neurons and parvalbumin-containing neurons. Exp. Brain Res. 92, 1–14.
Renteria, R., Baltz, E.T., Gremel, C.M., 2018. Chronic alcohol exposure disrupts top-down control over basal ganglia action selection to produce habits. Nat. Commun. 9, 211.
Reynolds, J.N.J., Wickens, J.R., 2000. Substantia nigra dopamine regulates synaptic plasticity and membrane potential fluctuations in the rat neostriatum, in vivo. Neuroscience 99, 199–203.
Ron, D., Wang, J., 2009. The NMDA receptor and alcohol addiction. In: VanDongen, A.M. (Ed.), Biology of the NMDA Receptor. CRC Press, Boca Raton, pp. 59–77.
Rudebeck, P.H., Walton, M.E., Smyth, A.N., Bannerman, D.M., Rushworth, M.F., 2006. Separate neural pathways process different decision costs. Nat. Neurosci. 9, 1161–1168.
Saxena, S., Brody, A.L., Schwartz, J.M., Baxter, L.R., 1998. Neuroimaging and frontal-subcortical circuitry in obsessive-compulsive disorder. Br. J. Psychiatry Suppl, 26–37.
Sciamanna, G., Ponterio, G., Mandolesi, G., Bonsi, P., Pisani, A., 2015. Optogenetic stimulation reveals distinct modulatory properties of thalamostriatal vs corticostriatal glutamatergic inputs to fast-spiking interneurons. Sci. Rep. 5, 16742.
Shen, W., Flajolet, M., Greengard, P., Surmeier, D.J., 2008. Dichotomous dopaminergic control of striatal synaptic plasticity. Science 321, 848–851.
Smith, J.B., Klug, J.R., Ross, D.L., Howard, C.D., Hollon, N.G., Ko, V.I., Hoffman, H., Callaway, E.M., Gerfen, C.R., Jin, X., 2016. Genetic-based dissection unveils the inputs and outputs of striatal patch and matrix compartments. Neuron 91, 1069–1084.
Volkow, N.D., Fowler, J.S., 2000. Addiction, a disease of compulsion and drive: involvement of the orbitofrontal cortex. Cerebr. Cortex 10, 318–325.
Volkow, N.D., Fowler, J.S., Wolf, A.P., Hitzemann, R., Dewey, S., Bendriem, B., Alpert, R., Hoff, A., 1991. Changes in brain glucose metabolism in cocaine dependence and withdrawal. Am. J. Psychiatr. 148, 621–626.
Volkow, N.D., Wang, G.J., Tomasi, D., Baler, R.D., 2013. Unbalanced neuronal circuits in addiction. Curr. Opin. Neurobiol. 23, 639–648.
Wall, N.R., De La Parra, M., Callaway, E.M., Kreitzer, A.C., 2013. Differential innervation of direct- and indirect-pathway striatal projection neurons. Neuron 79, 347–360.
Wall, N.R., Neumann, P.A., Beier, K.T., Mokhtari, A.K., Luo, L., Malenka, R.C., 2019. Complementary genetic targeting and monosynaptic input mapping reveal recruitment and refinement of distributed corticostriatal ensembles by cocaine. Neuron 104, 916–930 e915.
Wang, J., Ben Hamida, S., Darcq, E., Zhu, W., Gibb, S.L., Lanfranco, M.F., Carnicella, S., Ron, D., 2012. Ethanol-mediated facilitation of AMPA receptor function in the dorsomedial striatum: implications for alcohol drinking behavior. J. Neurosci. 32, 15124–15132.
Wang, J., Carnicella, S., Phamluong, K., Jeanblanc, J., Ronesi, J.A., Chaudhri, N., Janak, P.H., Lovinger, D.M., Ron, D., 2007. Ethanol induces long-term facilitation of NR2B-NMDA receptor activity in the dorsal striatum: implications for alcohol drinking behavior. J. Neurosci. 27, 3593–3602.
Wang, J., Cheng, Y., Wang, X., Roltsch Hellard, E., Ma, T., Gil, H., Ben Hamida, S., Ron, D., 2015. Alcohol elicits functional and structural plasticity selectively in dopamine D1 receptor-expressing neurons of the dorsomedial striatum. J. Neurosci. 35, 11634–11643.
Wang, J., Lanfranco, M.F., Gibb, S.L., Ron, D., 2011. Ethanol-mediated long-lasting adaptations of the NR2B-containing NMDA receptors in the dorsomedial striatum. Channels 5, 205–209.
Wang, J., Lanfranco, M.F., Gibb, S.L., Yowell, Q.V., Carnicella, S., Ron, D., 2010. Long-lasting adaptations of the NR2B-containing NMDA receptors in the dorsomedial striatum play a crucial role in alcohol consumption and relapse. J. Neurosci. 30, 10187–10198.
Wei, X., Ma, T., Cheng, Y., Huang, C.C.Y., Wang, X., Lu, J., Wang, J., 2018. Dopamine D1 or D2 receptor-expressing neurons in the central nervous system. Addiction Biol. 23, 569–584.
Wright, P., Albarracin, D., Brown, R.D., Li, H., He, G., Liu, Y., 2008. Dissociated responses in the amygdala and orbitofrontal cortex to bottom-up and top-down components of emotional evaluation. Neuroimage 39, 894–902.
Wydra, K., Suder, A., Borroto-Escuela, D.O., Filip, M., Fuxe, K., 2015. On the role of A(2) A and D(2) receptors in control of cocaine and food-seeking behaviors in rats. Psychopharmacology (Berlin) 232, 1767–1778.
Yamada, K., Kanemura, A., 2020. Simulating bout-and-pause patterns with reinforcement learning. PloS One 15, e0242201.
Young, J.J., Shapiro, M.L., 2009. Double dissociation and hierarchical organization of strategy switches and reversals in the rat PFC. Behav. Neurosci. 123, 1028–1035.